

## An Analytical Core Model for Tapered Tri-Gate Fin Field-Effect Transistors

Libin Liu<sup>a</sup>, Chunsheng Jiang<sup>a</sup>, Renrong Liang<sup>a</sup>, Jing Wang<sup>a</sup> and Jun Xu<sup>a</sup>

<sup>a</sup>*Tsinghua National Laboratory for Information Science and Technology, Institute of Microelectronics, Tsinghua University, Beijing 100084, People's Republic of China, junxu@tsinghua.edu.cn*

Recently, the Fin field-effect transistors (FinFETs) have been extensively investigated because of their excellent electrical performance [1]. Many analytical models have been proposed to describe the current-voltage characteristics of the rectangular tri-gate FinFETs. However, due to the limitation of the lithography and etching techniques, the channel of the manufactured FinFETs always have a taper-shaped instead of a rectangular-shaped as shown in Fig. 1 [2]. In this work, an analytical core model of the tapered tri-gate FinFETs is developed and its accuracy is verified by the numerical simulation using a 3D Sentaurus Device simulator.

An analytical core model has been proposed for the regular rectangular tri-gate FinFETs by assuming an arbitrary channel potential profile [3]. In this model, the charges (mobile charge density  $Q_e$  and depletion charge density  $Q_d$ ) in the channel and the device structure parameters (gate capacitance  $C_g$ , channel capacitance  $C_{ch}$  and area of channel  $A_{ch}$ ) approximately satisfy the Eq. (1). Respect to the rectangular FinFETs, the tapered tri-gate FinFETs has a wider fin bottom width ( $W_B$ ) respect to the fin top ( $W_T$ ). The  $C_g$ ,  $C_{ch}$ ,  $A_{ch}$  and  $Q_d$  of the tapered tri-gate FinFETs are not only a function of the fin width and fin height ( $H$ ), but also of the angle ( $\theta$ ) between the fin side and fin bottom. For the tapered tri-gate FinFETs, the  $C_g$  is estimated by the capacitance of a metal-insulator-metal (MIM) capacitor, which is obtained by replacing the channel with metal. The MIM is been divided into two parts combined in parallel: the top gate capacitor and the side gate capacitor. The top gate capacitor is treated as one-third of the square tri-gate capacitor with side-length  $W_T$ . The side gate capacitor is estimated by half of the square gate-all-around capacitor with side-length  $H/\sin\theta$ . So, utilizing the work of Ruiz [4], the  $C_{MIM}$  can be described by Eq. (2). A fitting parameter  $\gamma$  is included to optimize the model. As it is shown in Fig. 2 and Fig. 3 for a fixed  $\gamma=0.63$ ,  $C_{MIM}$  shows good accuracy compared with the simulation results in a wide range of  $W_B$ ,  $H$ ,  $T_{ox}$  and  $\theta$ . The  $C_{ch}$  is given by Eq. (4), in which the first and second terms are contributed by the two side gates and the top gate, respectively.  $A_{ch}$  and  $Q_d$  are described by Eqs. (5) and (6), respectively.

The  $Q_e$  can be solved from Eq. (1) for a certain bias condition. Then, the drain current of the tapered FinFET is obtained by analytically integrating  $Q_e$  from source to drain, as shown in Eq. (8) [5]. It has been found that the  $C_g$  can effectively affect the accuracy of the model and its value is underestimated by  $C_{MIM}$ . In fact, the  $C_g$  is far more complex than  $C_{MIM}$ . The control capability of the gate to the channel is enhanced by the geometry effects, such as the corner effects. So, it's obvious that the desired  $C_g$  should be bigger than  $C_{MIM}$ . Therefore, to ensure the accuracy of the model, parameter  $\beta$  is introduced to take the gate enhancement into account as indicated in Eq. (3).  $\alpha_n$  is another fitting parameter used to optimize the model [3]. By optimization, the  $\alpha_n$  and  $\beta$  is been fixed at 2.3 and 1.1, respectively. As shown in Fig. 4 and Fig. 5, the model shows good accuracy with the numerical simulation at a wide range of structures (different  $W_B$ ,  $H$ ,  $\theta$ ) and bias conditions ( $V_{DS}$ ,  $V_{GS}$ ).

In conclusion, an analytical core model of tapered tri-gate FinFETs is proposed. This model has an explicit and continuous expression in all the operation regimes. It shows good agreement with the numerical simulation for a wide range of device parameters and bias conditions.

This research was supported in part by the National Science and Technology Major Project (Grant Nos. 2009ZX02035-004-01 and 2011ZX02708-002), and by the National Natural Science Foundation of China (Grant No.61306105).

### References

- [1] B. Yu, et al, "FinFET scaling to 10 nm gate length," *Proc. IEDM*, Dec. 2002, pp. 251–254.
- [2] X. Wu, et al, "Impacts of nonrectangular fin cross section on the electrical characteristics of FinFET," *IEEE Trans. Electron. Device*. vol. 52, no. 1, pp. 63-68, Jan. 2005.

- [3] J. P. Duarte, et al, "A Universal Core Model for Multiple-Gate Field-Effect Transistors. Part I: Charge Model," *IEEE Trans. Electron. Device.* vol. 60, no. 2, pp. 840 - 847, Feb. 2013.
- [4] F. J. G. Ruiz, et al. "Equivalent Oxide Thickness of Trigate SOI MOSFETs with High-k Insulator," *IEEE Trans. Electron. Device.* vol. 56, no.11, pp. 2711-2719, Nov. 2009.
- [5] J. P. Duarte, et al. "A Universal Core Model for Multiple-Gate Field-Effect Transistors. Part II: Drain Current Model," *IEEE Trans. Electron. Device.* vol. 60, no. 2, pp. 848-855, Feb. 2013.

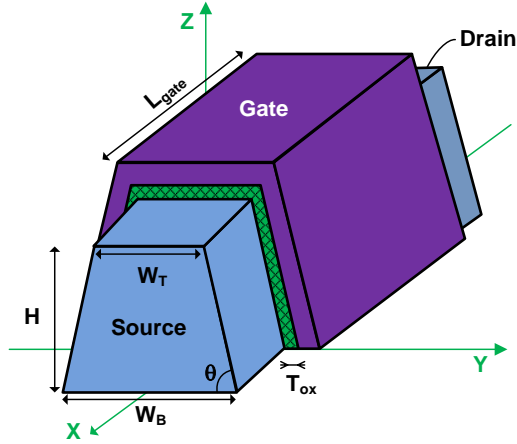


Fig. 1 Schematic diagram of the tapered tri-gate field effect transistor.

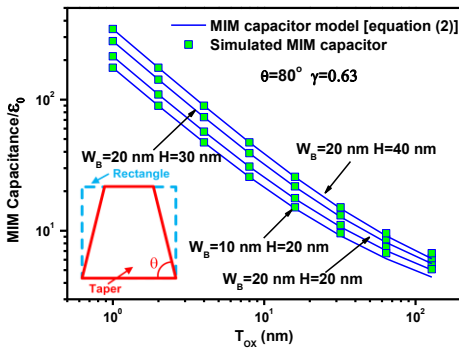


Fig. 2 Simulated capacitance of the tapered tri-gate MIM capacitor (symbol) as the function of the oxide thickness. Its comparison with the analytical model is also included (line). Inset: structure of the rectangular tri-gate (blue) used as a comparison of tapered tri-gate (red) and the definition of  $\theta$ .

Table. 1 The equations of the proposed model

$$V_{GS} - V_{FB} + \frac{Q_d}{C_g} - V = -\frac{Q_e}{C_g} + v_T \ln \left[ \frac{Q_e (Q_e / \alpha_n + Q_d) / v_T C_{ch}}{q A_{ch} \frac{n_i^2}{N_{ch}} \left( 1 - \exp \frac{Q_e / \alpha_n + Q_d}{v_T C_{ch}} \right)} \right] \quad (1)$$

$$C_{MIM} = \frac{5\gamma\epsilon_{ox}/2}{\ln(1+5\gamma t_{ox} \sin\theta/4H)} + \frac{3\gamma\epsilon_{ox}/2}{\ln[1+3\gamma t_{ox}/(W_B-2H/\tan\theta)]} \quad (2)$$

$$C_g = \beta C_{MIM} \quad (3)$$

$$C_{ch} = 2 \tan \theta \epsilon_{si} \ln \left( 1 - \frac{2}{\tan \theta} \right) + \epsilon_{si} \left( \frac{W_B}{H} - \frac{2}{\tan \theta} \right) \quad (4)$$

$$A_{ch} = H W_B - H^2 / \tan \theta \quad (5)$$

$$Q_d = -q N_{ch} A_{ch} \quad (6)$$

$$I_{DS} = -\frac{\mu}{L_{gate}} \int_{Q_{e,S}}^{Q_{e,D}} Q_e \frac{dV}{dQ_e} dQ_e \quad (7)$$

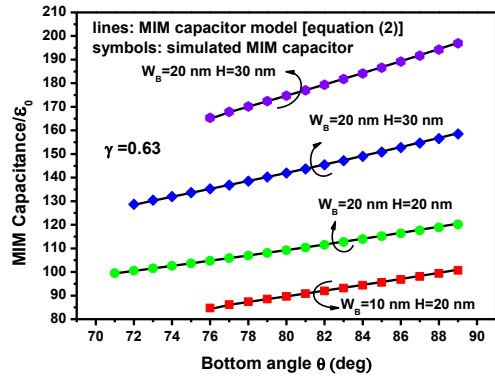


Fig. 3 The capacitance of the tapered tri-gate MIM capacitor  $\theta$  obtained from the analytical model (line) and the numerical simulation (symbol). Curves of different fin size are included.

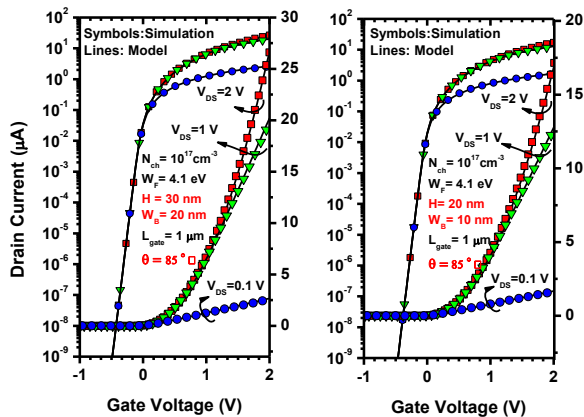


Fig. 4 The transfer characteristics of the tapered FinFET obtained from the proposed model and the numerical simulation. The  $\theta$  is the same but the size of the silicon fin is different for the left and right figure.

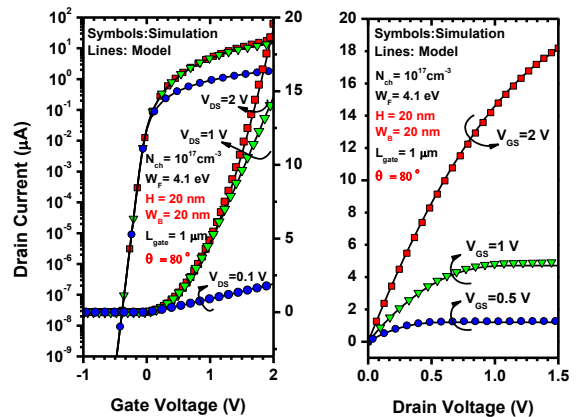


Fig. 5 The transfer characteristic (left) and output characteristic (right) of the tapered FinFET. The fin size is  $20 \times 20$  ( $W_B \times H$ , nm) and  $\theta = 80^\circ$ .